DC Dielectric Breakdown Behavior of Thermally Sprayed Ceramic Coatings

Minna Niittymäki[1], Tomi Suhonen[2], Jarkko Metsäjoki[2] & Kari Lahti[1]

[1]*Tampere University of Technology, Department of Electrical Engineering, Tampere, Finland*
[2]*Technical Research Centre of Finland, Espoo, Finland*

Abstract

Previous studies of dielectric properties of thermally sprayed insulating ceramic coatings are focused on linearly ramped dielectric breakdown strength as well as DC resistivity, relative permittivity and dielectric loss characterizations. However, reports of the effects of ramp rate or of any kind of long term stressing on the breakdown strength cannot be found in literature. The aim of this paper was to study the DC breakdown behavior of one type of HVOF sprayed alumina coating under different stresses. It can be concluded that the ramp rate of DC breakdown measurement has no remarkably influence on the breakdown strength. The breakdown behavior was also studied using step-by-step tests with two constant step voltages and step durations. The DC resistivity of the alumina coating showed strong dependence on the applied electric field. The resistivity behaved ohmicly below the field strength of ~0.5 V/µm and above ~8…12 V/µm, however, the resistivity decreased approximately three decades in the non-ohmic region (0.5 V/µm →). At electric field strengths above ~25 V/µm, the degradation started in the material leading to breakdown. However, when the step duration was longer (60 min), the degradation process started already slightly below the applied field of 25 V/µm.

1 Introduction

Thermally sprayed ceramic coatings can be used as an electrical insulation in demanding conditions such as in high temperature applications e.g. fuel cells. Thermal spraying as a method enables to manufacture insulating layer on a challenging geometry in quite inexpensive way. Despite of the clear needs for such insulating coatings, previous studies of the dielectric properties of thermally sprayed insulating ceramic coatings are focused on linearly ramped dielectric breakdown strength as well as DC resistivity, relative permittivity and dielectric loss characterizations [1]–[8]. Anyhow, reports of the effects of ramp rate or of any kind of longer term stressing on the breakdown strength cannot be found in literature. In some cases, the ramp rate is found to have an effect on the breakdown strength of certain insulation materials, with higher ramp rate giving higher breakdown strength for the material due to the space charge phenomena [9], [10].

The aim of this paper was to study the DC breakdown behavior of one type of thermally sprayed Al_2O_3 ceramic coating under different stresses as well as the permittivity, dielectric losses and DC resistivity of the coating. The breakdown behavior was studied with two different linear ramp rates and with stepwise breakdown tests varying the step size and duration enabling evaluations of the possible changes in the breakdown mechanisms.

The DC resistivity of thermally sprayed coatings has been reported to be non-ohmic when the electric field is increased above certain electric field (typically the level was only ~0.5 V/µm) [5], [6], [8]. However, DC resistivity has been measured previously only at electric field strengths varying from 0.1 V/µm to 5 V/µm due to the limitations of the measuring device used. In order to study the DC resistivity at higher electric fields, new measurement setup needed to be developed. In practice, a sensitive current measuring system was included in the stepwise breakdown measurements enabling the resistivity determination at each voltage level until the breakdown occurred.

In [8], the relative permittivity and loss index was studied as a function of electric field in order to investigate the effect of electric field on these properties. As a conclusion, especially the loss index is dependent on the electric field at low frequencies which is well in line with the previous studies focused on the non-ohmic behavior of DC resistivity [5], [6]. However, in this paper the focus is not on these properties and thus relative permittivity and loss index were measured only at one electric field strength.

2 Experimental

2.1 Studied Material

Commercial Al_2O_3 powder was sprayed using high-velocity-oxygen-fuel (HVOF) technique on stainless steel substrate. The powder particle size varied from 7 µm to 29 µm which is a typical range for ceramic powders used in HVOF spraying. In the spraying process the powder particles are heated and accelerated towards the substrate, the melted particles form droplets which hit the substrate or coating surface forming a coating consisting of splats with interfaces in between. The surfaces of the splats cool down faster than the internal parts and due to this the surfaces are normally more amorphous areas, while the internal parts are typically crystalline. These splats form the lamellar structure of a coating while the coating exhibits also defects e.g. voids as well as some cracks. During the cooling at least some vertical cracks are rather easily formed in the coating, and these are problematic for electrical insulation materials. However, thermally sprayed coatings exhibit quite typically at least some vertical cracks and the length and amount of the cracks

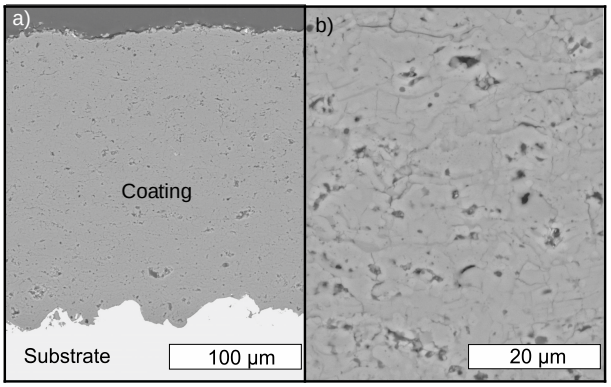

Figure 1 – SEM/BSE micrograph images of a cross-section of the studied alumina coating, with magnifications of 200 (**a**) and 1000 (**b**).

play an important role. The lamellar microstructure of the studied coating can be seen in the Figure 1.

The coating thicknesses of the samples were defined by magnetic measuring device (Elcometer 456B) as well as from cross-section surface images taken by optical micrographs [7]. In the magnetic measurements the mean values and the experimental standard deviations of the thicknesses were calculated from 10 parallel measurements covering the electrode area used in the DC resistivity and dielectric spectroscopy measurements (Table 1).

Porosity of the coatings were defined by image analysis from optical micrographs (OM) and from scanning electron microscope (SEM) images using secondary electron (SE) and backscattering electron (BSE) detectors [7] (Table 1). While making the image analysis from the SEM figures, some problems occurred and due to this the obtained porosity values are most probably too small, however, the values are given as a reference in Table 1. In addition to above, the gas (nitrogen) permeability of the coating is also presented in Table 1. Typically, high gas permeability value of a material indicates high porosity. The OM porosity of the studied alumina coating is notably higher (6 %) than the porosities of the HVOF alumina coatings in [8] where the porosity values were below 2 %. The gas permeabilities of the coatings in [8] were 5.7 nm^2 and 19.2 nm^2 while in this paper the gas permeability is 11.1 nm^2. Thus, the gas permeability values probably give more realistic view of the actual porosity of the material.

Table 1 – Porosity and thickness of the studied coating defined by using various methods as well as the gas (nitrogen) permeability of the material.

Thickness (µm)	From magnetic. meas	228
	SD	6.2
	From cross-section image	215
Porosity (%)	OM	6.0
	SEM/SE	1.7
	SEM/BSE	3.7
Gas permeability (nm^2)		11.1

2.2 Sample Preparation and Test Procedures

For the DC resistivity and relative permittivity measurements, a round silver electrode (∅=50 mm) was painted on the middle of a coating sample after the thickness measurements. In addition, a shield electrode was painted around the measuring electrode to neglect possible surface currents. For breakdown measurements silver electrodes (∅=11 mm) were painted on the sample surface to improve the contact between the voltage electrode and the coating. The used silver paint (SPI Conductive Silver Paint) was studied not to penetrate into the coating [7]. After painting the electrodes the samples were at first dried at 120 °C for two hours followed by conditioning at climate room at 20 °C, RH 20 % for at least 12 h before the measurements. All measurements for the samples were also performed in climate room at the above mentioned conditions.

2.3 Relative Permittivity and Dielectric Losses

Relative permittivity and dielectric losses of the material were studied with an insulation diagnosis analyzer device (IDA 200, U_{max}=200 V_{peak}). During the measurements, a sinusoidal voltage with varying frequency was applied over the sample. The measuring electric field strength was 0.88 V_{peak}/µm equaling the voltage of 200 V_{peak}.

The complex impedance of a sample was calculated from the measured test voltage and the current through a sample which was expressed by IDA device as the equivalent parallel RC circuit model. The relative permittivity (ε_r) and dissipation factor (*tan* δ) were calculated from the measured parallel resistance and capacitance using Eq. (1)-(2), where C_p is measured parallel capacitance and R_p parallel resistance of the equivalent circuit. C_0 is the so-called geometric capacitance of the test sample (vacuum in place of the insulation) and ω is the angular frequency. The edge field correction (C_e) was not used because the shield electrode was utilized in the measurements. Loss index (ε_r'') includes all the losses of a sample: both conductive and dielectric ones. It can be defined from relative permittivity and dissipation factor, *tan* δ, with Eq. (3). All the test arrangements were performed in accordance with the IEC standard 60250 [11].

$$\varepsilon_r \approx \varepsilon_r' = \frac{C_p}{C_0} - \frac{C_e}{C_0} \quad (1)$$

$$\tan\delta = \frac{1}{R_p C_0 \omega} \quad (2)$$

$$\varepsilon_r'' = \varepsilon_r \tan\delta \quad (3)$$

2.4 DC Resistivity

Resistivity measurements were made using Keithley 6517B electrometer. The test voltage was maintained until a stabilized current level (i.e. pure resistive current) was reached. In practice, the tests were performed at test voltages ranging from 10 V to 1000 V

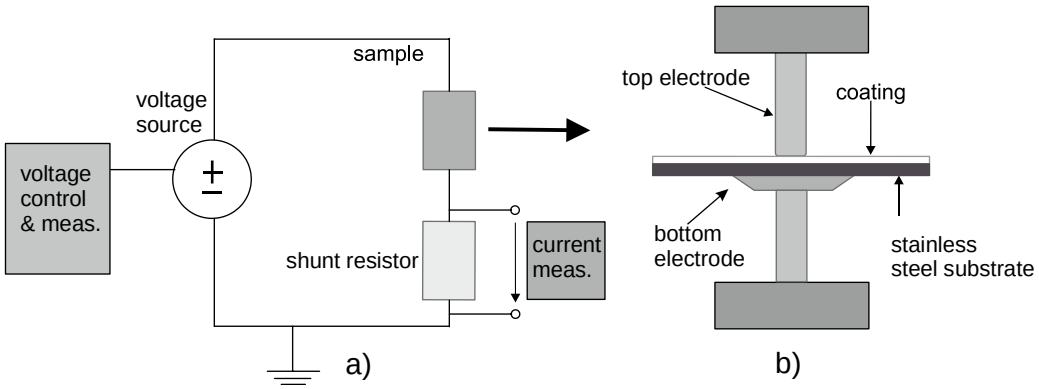

Figure 2 – The schematic figure of the measurement circuit used in the stepwise breakdown tests.

in order to study the resistivity as a function of electric field. The stabilized DC current was measured 1000 s after the voltage application. The resistivity was defined from the test voltage, the stabilized current, electrode geometry and sample thickness. All the measuring arrangements were in accordance with the standards IEC 60093/ASTM D257-07 [12], [13]. In addition to the electrometer measurements, resistivities of the coatings at higher field strengths were determined based on the current measurements made during the stepwise breakdown measurements (details in Section 2.5).

2.5 DC Breakdown Strength

DC breakdown measurements were performed either with linearly or stepwise increased DC voltage. Oil immersion was not used in the measurements because the coatings are porous allowing oil to penetrate into the coating which significantly affects the breakdown strength [7]. During the breakdown (BD) tests, the samples were clamped between two stainless steel electrodes: a flat-ended rod (∅= 11 mm) and a flat plate (∅=20 mm).

A software controlled linear ramp rate of 100 V/s or 1000 V/s was used throughout the ramp tests until breakdown occurred [7]. Dielectric breakdown strength (DBS) of a coating was calculated dividing the breakdown voltage by the corresponding coating thickness at the painted electrode (∅=11 mm) location.

The stepwise measurements were made with two different step durations, 6 min and 60 min. The 6 min step tests were started at the voltage level of 250 V which was the step size as well. The 60 min step measurements were started at the voltage of 4000 V (~18.6 V/µm) while the step size was 500 V. The schematic figure of the measurement circuit is presented in Figure 2. The current was measured throughout the test with the help of shunt resistor which was either 1 MΩ or 10 kΩ depending on the signal level and the signal was measured with Keithley 2001 DMM. The voltage source was Keihtley 2290-10 power supply (U_{max}=10 kV).

3 Results and Discussion

3.1 Relative Permittivity and Dielectric Losses

Figure 3 presents the relative permittivity and the loss index of the studied coating as a function of frequency at the electric field of 0.88 V_{peak}/µm. The relative permittivity is 11.7 at the frequency of 50 Hz and the loss index at the same frequency is 3.4. These values are quite typical for HVOF sprayed alumina coatings at dry ambient conditions [4], [8].

3.2 DC Resistivity

DC resistivity was defined as a function of electric field which was varied from 0.04 V/µm to 4.4 V/µm. The resistivity as a function of electric field can be seen in Figure 4a. It can be observed that the resistivity is practically ohmic when the applied field is below 0.5 V/µm and above that the resistivity decreases non-ohmicly as reported in [5]–[7], [8].

Because the maximum voltage of Keithley electrometer is 1 kV and the coatings are typically approximately 200 µm thick, it was not possible to measure the DC conductivity above the electric field strengths of approximately 5 V/µm with this device. Thus, a new measurement setup was developed in order to study the DC resistivity behavior of thermally sprayed coatings up to the breakdown field strengths. In practice, the current and the voltage was measured and recorded during the stepwise breakdown tests allowing

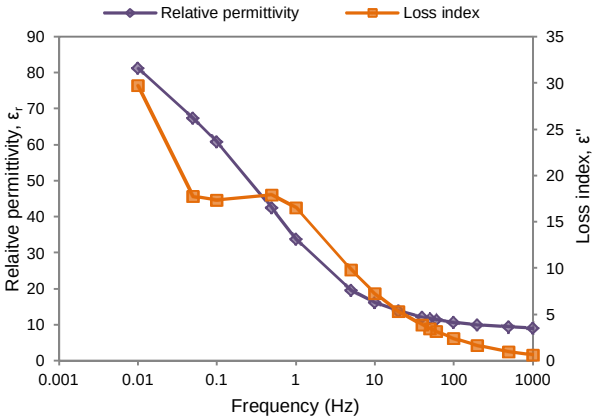

Figure 3 – The relative permittivity and the loss index of the studied material as a function of frequency.

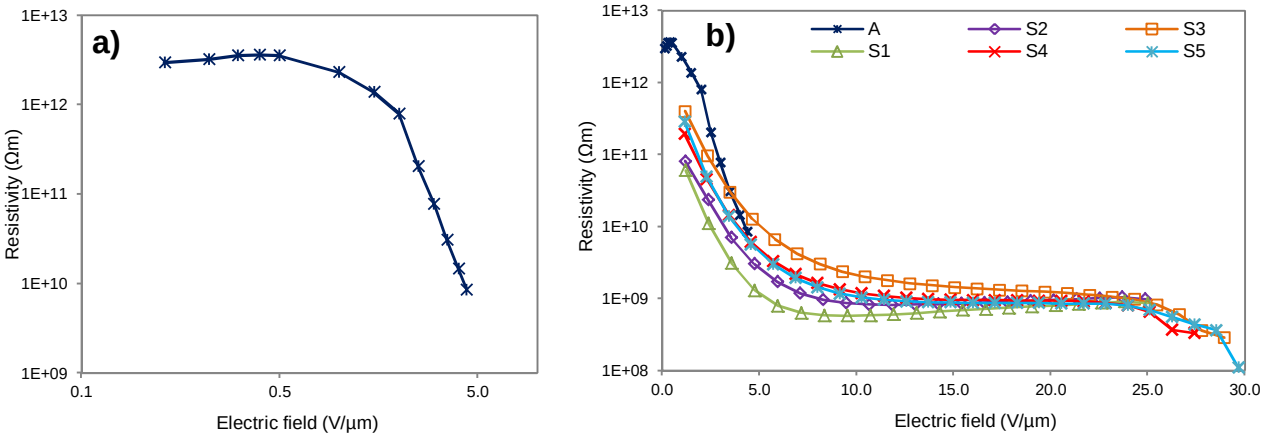

Figure 4 – **a)** DC resistivity of the studied coating (sample A) as a function of electric field (log-log-axis). **b)** DC resistivities of all the samples as a function of electric field (y-axis is logarithmic).

an estimation of DC resistivity to be made at higher field strengths. It is considered as estimation because typically the DC current did not fully stabilize during the 6 min measurement periods. Anyhow, the estimations are rather good (i.e. currents were close to the stabilized levels). Naturally, the resistivies were defined at the end of each step. This DC resistivity as a function of electric field is presented in Figure 4b.

It can be noticed from Figure 4b that the resistivity of the studied coating can be divided to certain operating areas. The resistivity was ~10^{12} Ωm and in ohmic region when the applied electric field was below 0.5 V/µm (Figure 4b). When the applied field was from 0.5 V/µm to 8…12 V/µm, the resistivity was in the non-ohmic region and decreased approximately three decades (Figure 4b). At the field strengths from 8…12 V/µm to 25 V/µm the resistivity was settled to ~10^{9} Ωm, (except in case of sample S3). When the applied field was close to the breakdown strength, the resistivity started to slightly decrease which can be seen in Figure 4b indicating an initiation of degradation/pre-breakdown process approximately from 25 V/µm.

Typically DC resistivity of insulating materials is defined at quite low voltage level (below 1 kV) but due to the shown behavior this can lead in erroneous indication of the material property since the behavior at higher service field strengths can be evidently different. Thus, better estimation of the DC resistivity of thermally sprayed ceramic coating can be defined when the applied electric field is above 10 V/µm or at service stress level of the material.

3.3 DC Breakdown Strength

3.3.1 Ramp tests

When the ramp rate was 100 V/s, the mean breakdown strength of 10 parallel measurements was 29.7 V/µm while the corresponding experimental standard deviation was 1.5 V/µm. At 10 times higher ramp rate (1000 V/s), the mean breakdown strength was 31 V/µm (SD=2.4 V/µm). It can be concluded that the ramp rate has no significant effect on the breakdown strength of these thermally sprayed ceramics because the breakdown strengths of different ramping rates are almost in the range of the standard deviations and thus the effects due to e.g. space charge accumulation cannot be noticed. The breakdown strength of the studied coating (ramp rate 100 V/s) is at similar level to the strengths obtained in previous studies [4], [7], [8] for HVOF sprayed alumina coatings.

3.3.2 Step tests

The step-by-step tests were carried out with 6 min and 60 min step durations. Table 2 presents the breakdown strength and total duration of each these tests. In addition, the mean and experimental standard deviations from five parallel DBS tests are given. The step voltage was two times higher in the 60 min tests than in 6 min tests, decreasing the 'resolution' of the 60 min tests. In the 60 minute tests the total stress duration of the samples varied from 100 min to 236 min. In the 6 min tests this variation was from 121 min to 159 min. Thus, the total duration was at quite similar level in both test types.

During the stepwise breakdown measurements certain problems took place in the one hour tests and thus all the recorded current data were not valid. Due to this, Figure 5a presents only the currents measured for the samples L2, L3 and L5 as a function of time.

As it was discussed earlier in Section 3.2, a kind of

Table 2 – Breakdown strength of the studied alumina coating in step-by-step tests. The step duration was 6 min for S-samples and 60 min for the L-samples.

Sample	DBS (V/µm)	Time to breakdown	Mean (V/µm)	SD (V/µm)
S1	25.0	121 min	27.2	2.0
S2	24.9	121 min		
S3	28.9	152 min		
S4	27.4	145 min		
S5	29.7	159 min		
L1	27.36	182 min	23.9	2.3
L2	22.83	144 min		
L3	20.27	100 min		
L4	24.77	236 min		
L5	24.12	187 min		

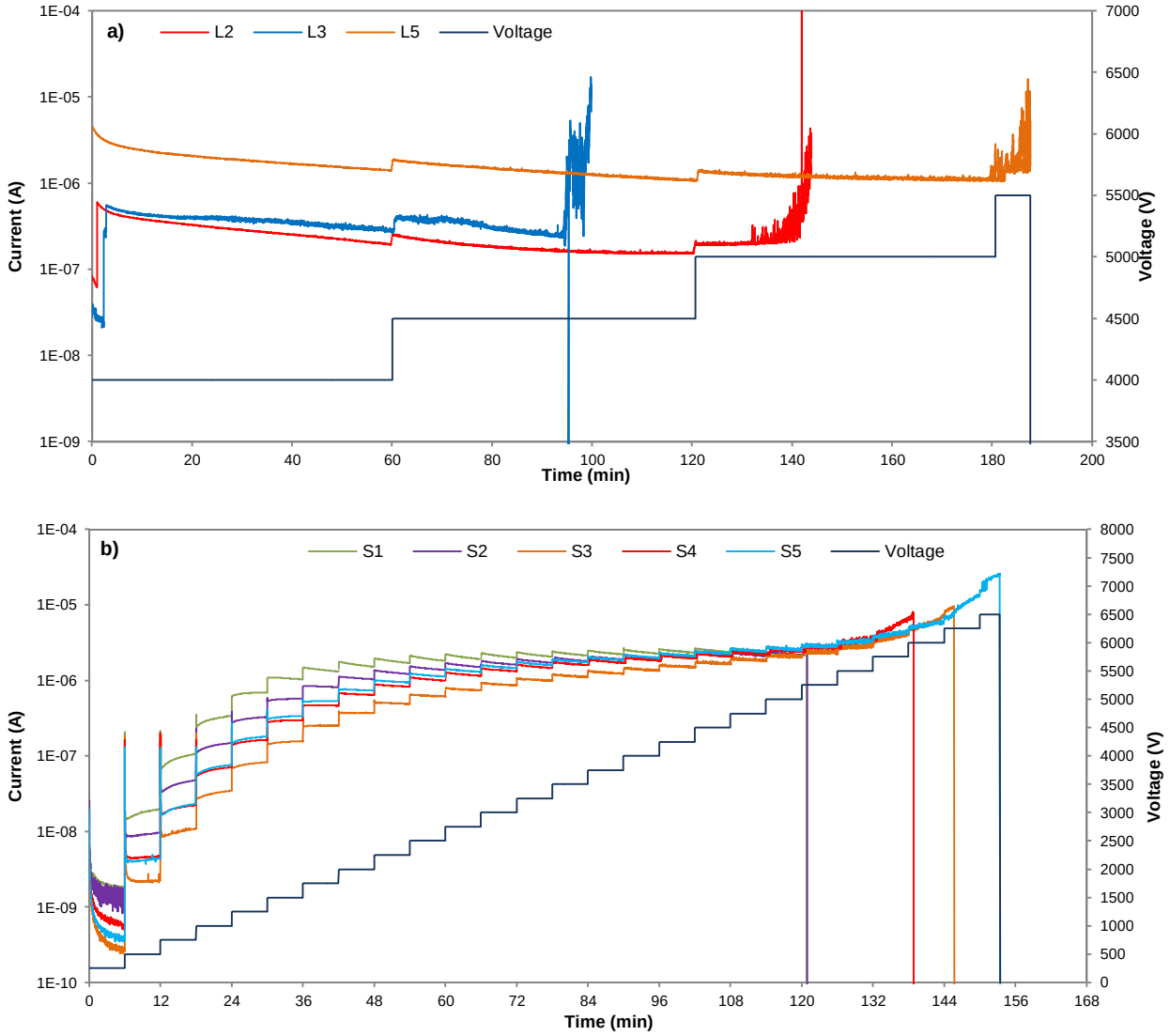

Figure 5 – **a)** Measured DC current of the studied material samples as well as the step-by-step voltage, when the step duration was 60 min, step voltage 500 V and the test was started at the voltage level of 4 kV. **b)** Measured DC currents as a function time during the 6 min/250 V step test with a start level of 250 V.

degradation/failure process started typically before the studied thermally sprayed alumina coating broke down which can be seen as a decrease in DC resistivity (Figure 4b). This same behavior can also be noticed in the 60 min step tests when the current started to increase approximately two minutes before the samples broke down (Figure 5a). It can also be noticed from the Figure 5a that the samples L2 and L5 have quite similar behavior throughout the test although their current levels and the breakdown strength differed. The currents of these two samples seemed to stabilize during the last full steps, 4.5 and 5.0 kV, respectively. On the third step (5 kV), the current of L2 was stable until the degradation started two minutes before the breakdown. A quite similar process took place for the sample L5 after increasing the test voltage to 5.5 kV. During this failure process, the resistivity of samples L2 and L5 decreased approximately one decade before the final breakdown. Similar decrease was also seen, especially, in the resistivity of sample S5 tested in 6 min step test (Figure 4b). Although sample L3 had almost similar degradation process just before the breakdown, the current started to slightly increase already in the middle of the first voltage step (4 kV). Thus, some kind of failure process started already at this point and continued on the second step (4.5 kV) The final current increase started 2 min before the breakdown.

3.4 Further Discussion of the Field Dependent Behavior of the Coating

Figure 4b presented the DC resistivity as a function of electric field and Figure 5b shows the corresponding DC currents of 6 min step tests. As it was discussed earlier, the DC resistivity behavior of the studied coating can be divided into different areas:

- electric field below 0.5 V/µm: the resistivity behaves ohmicly, ~ 10^{12} Ωm

- electric field from 1 V/µm to 8…12 V/µm: the resistivity behaves non-ohmicly
- electric field from 8…12 V/µm to 25 V/µm: the resistivity behaves ohmicly at a new region, ~10^9 Ωm
- electric field above ~25 V/µm: degradation/pre-breakdown region

From Figure 5b it can be noticed that the currents of all S-samples stabilized at the first step (~ 1 V/µm) in the end of the measurement period although the values are different. At the second step (~ 2 V/µm) the currents of samples S3 and S4 stabilized while the currents of the other samples started to gradually increase. At the higher voltage levels, all the currents were not stabilized during the measurement periods indicating that the material was in the non-ohmic region. The currents settled at quite similar level when the applied field was 8…12 V/µm. The currents of samples S3-S5 started to gradually increase when the field reached to 25 V/µm. This similar behavior can be noticed in DC resistivity as a decrease (Figure 4b). Breakdown strength of samples S1 and S2 was 25 V/µm and the degradation process was not seen for these samples. Also, these two samples had higher current levels than the other samples during the whole test duration.

It seems that above the electric field strength of 25 V/µm the current started to gradually increase in case of all samples before the breakdowns occurred in the 6 min step tests. If the breakdown strength of the sample was 25 V/µm, no degradation before the breakdown can be seen. Based on this small set of results, the 25 V/µm may be seen as a kind of coating microstructure specific limit for the final degradation of this coating. However, when the step duration was longer (60 min), the degradation process started already below the 25 V/µm. Thus, the maximum possible service stress level for the studied thermally sprayed coating might be from ~10 V/µm to ~20 V/µm at most (taking not into account safety margins). Naturally, further long-term ageing tests are needed for more confident result.

4 Conclusions

The ramp rate in DC breakdown measurement has no significant effect on the breakdown strength of HVOF sprayed alumina coating. The breakdown behavior was also studied with increasing the voltage step-by-step with two constant step voltages and step durations. The DC resistivity was also defined from the shorter step duration tests. The DC resistivity of the alumina coating showed strong dependence on the applied electric field. The resistivity behaved ohmicly below ~0.5 V/µm and above ~8…12 V/µm, however, the resistivity decreased approximately three decades in the non-ohmic region (~0.5V/µm – ~8...12 V/µm). At electric field strengths above 25 V/µm, the degradation started in the material leading to breakdown. However, when the step duration was longer (60 min), the degradation process started already slightly below the applied field of 25 V/µm.

References

[1] L. Pawłowski, "The relationship between structure and dielectric properties in plasma-sprayed alumina coatings," *Surf. Coatings Technol.*, vol. 35, no. 3–4, pp. 285–298, 1988.

[2] F.L. Toma, S. Scheitz, L. M. Berger, V. Sauchuk, M. Kusnezoff, and S. Thiele, "Comparative study of the electrical properties and characteristics of thermally sprayed alumina and spinel coatings," *J. Therm. Spray Technol.*, vol. 20, no. 1–2, pp. 195–204, 2011.

[3] F.L. Toma, L. M. Berger, S. Scheitz, S. Langner, C. Rödel, A. Potthoff, V. Sauchuk, and M. Kusnezoff, "Comparison of the Microstructural Characteristics and Electrical Properties of Thermally Sprayed Al 2O 3 Coatings from Aqueous Suspensions and Feedstock Powders," *J. Therm. Spray Technol.*, vol. 21, no. 3–4, pp. 480–488, 2012.

[4] M. Niittymäki, B. Rotthier, T. Suhonen, J. Metsäjoki, and K. Lahti, "Effects of ambient conditions on the dielectric properties of thermally sprayed ceramic coatings," in *Proceedings of the 23th Nordic Insulation Symposium Nord-IS 2013*, 2013, pp. 131–135.

[5] M. Niittymäki, K. Lahti, T. Suhonen, U. Kanerva, and J. Metsäjoki, "Dielectric properties of HVOF sprayed ceramic coatings," in *Proceedings of the IEEE International Conference on Solid Dielectrics*, 2013, pp. 389–392.

[6] M. Niittymäki, T. Suhonen, J. Metsäjoki, and K. Lahti, "Influence of Humidity and Temperature on the Dielectric Properties of Thermally Sprayed Ceramic MgAl2O4 Coatings," in *2014 Annual Report Conference on Electrical Insulation and Dielectric Phenomena*, 2014, pp. 94–97.

[7] M. Niittymäki, K. Lahti, T. Suhonen, and J. Metsäjoki, "Dielectric Breakdown Strength of Thermally Sprayed Ceramic Coatings: Effects of Different Test Arrangements," *J. Therm. Spray Technol.*, vol. 24, no. 3, pp. 542–551, Jan. 2015.

[8] M. Niittymäki, T. Suhonen, J. Metsäjoki, and K. Lahti, "Electric Field Dependency of Dielectric Behavior of Thermally Sprayed Ceramic Coatings," in *2015 IEEE 11th International Conference on the Properties and Applications of Dielectric Materials (ICPADM)*, 2015, (submitted).

[9] G. Chen and J. Zhao, "Space charge and thickness dependent dc electrical breakdown of solid dielectrics," in *2012 International Conference on High Voltage Engineering and Application*, 2012, pp. 12–15.

[10] G. Chen, J. Zhao, S. Li, and L. Zhong, "Origin of thickness dependent dc electrical breakdown in dielectrics," *Appl. Phys. Lett.*, vol. 100, no. 22, p. 222904, 2012.

[11] "IEC standard 60250 Recommended methods for the determination of the permittivity and dielectric dissipation factor of electrical insulating materials at power, audio and radio frequencies including metre wavelengths," no. IEC Standard 60250. IEC, 1969.

[12] "IEC standard 60093 Methods of test for volume resistivity and surface resistivity of solid electrical insulating materials," no. IEC Standard 60093. IEC, 1980.

[13] "ASTM Standard D257 - 07 Standard Test Methods for DC Resistance and Conductance of Insulating Materials," no. ASTM Standard D257–07. ASTM International, West Conshohocken, PA, 2007.